J. Fluid Mech. (1976), *vol.* 75, *part* 4, *pp.* 737–749
Printed in Great Britain

Experiments to investigate transport processes in the near wakes of disks in turbulent air flow

By W. HUMPHRIES AND J. H. VINCENT
Department of Applied Physics, University of Strathclyde, Glasgow

(Received 22 January 1976)

Experiments reported previously determined the detention time of airborne smoke particles momentarily trapped in the wake bubble behind a flat disk normal to smooth air flow. The dimensionless group H, the product of the detention time t_d and mainstream air velocity U divided by the disk diameter D, was found to be 7·44 for all combinations of U, D and the Reynolds number, a result that was consistent with a suggested physical model for particle transport across the bubble boundary. The work is now extended into the regime of turbulent free-stream flow, where H is seen to decrease with an increasing level of turbulence while the base pressure coefficient becomes more negative. At the same time, the length of the bubble decreases, as does the bubble shape factor (the ratio of bubble volume to surface area, non-dimensionalized with respect to D). A simple theoretical relationship between H and the base pressure coefficient is argued, and is found to be in good agreement with experiment.

An important conclusion from this work is that the free-stream turbulence parameter $\Lambda \equiv l_f k_f^{\frac{1}{2}}/DU$ (where l_f and k_f are the length scale and the kinetic energy of the free-stream turbulence respectively) controls the properties of the flow about the disk.

This work has potential applications in several areas of topical technological interest.

1. Introduction

The flow of air about flat disks does not appear to have been as extensively studied as that about some other bluff obstacles (notably cylinders and rectangular flat plates), despite the fact that, from a purely physical point of view, the axisymmetric properties of the flow seem to provide a satisfying configuration in which to investigate many of the basic fluid mechanical processes common to most bluff-body flows. It could be argued that this relative neglect is due to the fact that an understanding of the flow about a disk has few engineering applications in itself. However a select body of literature has accumulated. For example, the main features of the flow about a flat disk normal to an airstream have been studied experimentally by Fail, Lawford & Eyre (1959) and Carmody (1964), who showed quantitatively how the fluid separates at the edge of the disk to form a turbulent mixing layer which spreads out downstream from and closes behind the disk to enclose a region of recirculatory flow (the *bubble*). The limiting streamline which separates the recirculatory flow from the mainstream flow (the *bubble* *boundary*) extends between two and three disk diameters downstream from the plane of the disk. The mean velocity of backflow inside the bubble is about 40 % of the mainstream velocity, and the mean velocity of turbulent fluctuations in the mixing layer over the bubble boundary is about 20 % of the mainstream velocity. Vortex shedding is present, but is less marked than in the case of two-dimensional bluff-body flows, and it is reasonable for most purposes to assume stability.

Experiments have recently been reported (Humphries & Vincent 1976) which investigated the transport of airborne scalar entities in the vicinity of the wake bubbles behind disks suspended in the working section of a low-speed, low-turbulence wind tunnel. Experiments were carried out using a conventional wind-tunnel smoke generator to supply smoke for injection axially into the airstream just upstream of the disks. Using a laser transmissometer to monitor the smoke trapped in the wake bubble, the dimensionless quantity $H \equiv Ut_d/D$ was determined experimentally, where t_d is the time constant of the exponential decay of the smoke trapped in the bubble following abrupt removal of the smoke source (the *detention* time), U the mainstream air velocity and D the disk diameter. The number H was found to be 7·44 for all U and D and all Reynolds numbers Re in the range 2000–40 000. This result was seen to be consistent with a physical model which describes the turbulent transport of airborne scalar entities (by an exchange mechanism suggested by Launder & Spalding 1972, p. 62) across the closed bubble boundary, making use of empirical data published by Carmody (1964).

In the present paper we describe experiments in which this work is extended to examine the effects of free-stream turbulence. The work is part of a wider programme to investigate the transport and precipitation of airborne particulates in flows with regions of recirculation, and to consider potential applications in air-pollution control devices and systems. Other possible applications of the work so far are envisaged in heat transfer, chemical engineering and architectural aerodynamics.

2. Theory

For a reasonably general description of the entrapment of scalar entities in the wake bubble behind a disk, consider the following variables.

D Disk diameter

U Mainstream air velocity

k_c Characteristic energy of turbulence for the fluid along the bubble boundary

k_{sc} Corresponding characteristic energy for the scalar

k_f Energy of free-stream turbulence

l_c Characteristic length scale of turbulence for the fluid along the bubble boundary

l_{sc} Corresponding characteristic length scale for the scalar

l_f Length scale of free-stream turbulence

μ Molecular viscosity of the fluid

ρ Density of the fluid
D_B Molecular diffusion coefficient for the scalar
f Frequency of vortex shedding

It is reasonable to assume that molecular diffusion and vortex shedding are of negligible importance over the range of conditions of interest. For smooth flow, k_c and l_c are determined by combinations of D, U, μ and ρ. With non-zero free-stream turbulence, k_c and l_c are also influenced by k_f and l_f. If the fluid carries a scalar it is convenient to introduce the corresponding quantities k_{sc} and l_{sc} to describe the motion of that scalar in the vicinity of the bubble boundary without having to specify any further details about its physical properties. In this way the analysis is not restricted to any particular type of scalar (notwithstanding our already declared interest in aerosols). In the simplest case, for scalar entities which move essentially as the fluid (for example, very small smoke particles), k_{sc} and l_{sc} become k_c and l_c respectively and are therefore determined solely by combinations of D, U, μ, ρ, k_f and l_f. The characteristic detention time during which a given typical entity is trapped inside the bubble boundary can therefore be written in terms of only six variables, thus

$$t_d = \phi_1\{D, U, \mu, \rho, k_f, l_f\}, \tag{1}$$

which by dimensional analysis leads to

$$H = F_1\{Re, l_f/D, k_f/U^2\}, \tag{2}$$

where $Re = DU\rho/\mu$, the Reynolds number.

From Humphries & Vincent (1976) we have an expression for H based on a physical model of the wake bubble for zero free-stream turbulence. For a scalar which behaves essentially like the fluid itself, this becomes

$$H = f_1(Re) f_2\left(Re, \frac{l_c}{D}, \frac{k_c}{U^2}\right) \Big/ (2b)^{\frac{1}{2}} \frac{l_c k_c^{\frac{1}{2}}}{DU}, \tag{3}$$

where b is the fraction of the kinetic energy of turbulent motion of the scalar carried in directions normal to the bubble boundary. The function f_1 is a bubble shape factor equal to the ratio of bubble volume to surface area (normalized with respect to disk diameter), and appears in order to allow for variations in the mean-flow streamline pattern. Although for smooth flow it is specified as a function of Re, it is in practice constant for Re greater than about 1000. However, when free-stream turbulence mixes with the wake turbulence, the effect is to produce extra entrainment of fluid out of the bubble and so shorten its length. Therefore it is more correct to write the shape factor as $f_1\{Re, l_f/D, k_f/U^2\}$. Further, since we are dealing with a mixing process which involves essentially the diffusion of fluid, it seems reasonable to lump together the two turbulence characteristics in the form of an effective turbulence diffusion coefficient (Prandtl 1945), and so rewrite the shape factor as $f_1\{Re, l_f k_f^{\frac{1}{2}}/DU\}$.

The function f_2 is the non-dimensionalized length scale indicating the mean distance across the bubble boundary over which the concentration of the scalar drops to zero on the outside. Consider an analogy with the simplest case of the diffusion of entities from a point source, where the mean distance diffused in a given time is a simple function of the diffusion coefficient. It is therefore reasonable to rewrite f_2 in the form $f_2\{Re, l_c k_c^{\frac{1}{2}}/DU\}$. If we now make the assumption that the product $l_c k_c^{\frac{1}{2}}$ is determined only by some combination of $l_f k_f^{\frac{1}{2}}$, D, U, μ and ρ, then this becomes $f_2\{Re, l_f k_f^{\frac{1}{2}}/DU\}$.

Incorporating these assumptions into (3) gives

$$H = F_2\{Re, l_f k_f^{\frac{1}{2}}/DU\}, \tag{4}$$

which is consistent with the dimensional analysis. It has been shown experimentally for smooth flow that H is independent of Re over a wide range of values. If the same can be shown to be true for turbulent flow, then

$$H = F_3\{l_f k_f^{\frac{1}{2}}/DU\}. \tag{5}$$

For the flow about a flat disk, the resultant turbulent mixing layer entrains fluid from the bubble and so sustains a base pressure p_b on the rear face of the disk which is lower than the free-stream static pressure p_s. Therefore we might expect the pressure difference $p_b - p_s$ to be closely related in some way to the detention time t_d. It can at least be described by the same set of variables, thus

$$p_b - p_s = \phi_2\{D, U, \mu, \rho, l_f, k_f\}, \tag{6}$$

which by dimensional analysis leads to

$$C_{pb} \equiv \frac{p_b - p_s}{\frac{1}{2}\rho U^2} = G_1\left\{Re, \frac{l_f}{D}, \frac{k_f}{U^2}\right\}, \tag{7}$$

where C_{pb} is the base pressure coefficient.

Now consider the wake region physically. Turbulent energy is produced by the disk at the expense of the mainstream motion and is transmitted through the fluid by diffusion, convection and viscous transport. All this energy is eventually converted into heat by viscous dissipation. The non-dimensional rate of production of turbulent energy within a volume of integration can be written in cylindrical co-ordinates as (Rouse 1960)

$$P = 4\iint\left\{\frac{\overline{u'v'}}{U^2}\left(\frac{\partial\bar{u}/U}{\partial r/R} + \frac{\partial\bar{v}/U}{\partial x/R}\right) + \frac{\overline{u'^2}}{U^2}\frac{\partial\bar{u}/U}{\partial x/R} + \frac{\overline{v'^2}}{U^2}\frac{\partial\bar{v}/U}{\partial r/R} + \frac{\overline{w'^2}}{U^2}\frac{\bar{v}/U}{r/R}\right\}\frac{r}{R}\frac{dr}{R}\frac{dx}{R}, \tag{8}$$

where R is the disk radius, where u', v' and w' are the axial, radial and tangential components of the velocity of the turbulent fluctuations respectively, and where $\bar{u}$ and $\bar{v}$ are the axial and radial components of the mean velocity (there is no tangential component). If we assume that

$$\frac{\partial\bar{u}}{\partial r} \gg \frac{\partial\bar{v}}{\partial x}, \frac{\partial\bar{u}}{\partial x}, \frac{\partial\bar{v}}{\partial r}, \frac{\bar{v}}{r},$$

based on inspection of the experimental data of Carmody (1963), then (8) simplifies to

$$P \sim 4\iint\frac{\overline{u'v'}}{U^2}\frac{\partial\bar{u}/U}{\partial r/R}\frac{r}{R}\frac{dr}{R}\frac{dx}{R}. \tag{9}$$

This is equal to the rate at which the disk does work on the fluid (non-dimensionalized), so that

$$C_D \equiv \frac{\text{force/area}}{\frac{1}{2}\rho U^2} \sim 4\iint \frac{\overline{u'v'}}{U^2}\frac{\partial\bar{u}/U}{\partial r/R}\frac{r}{R}\frac{dr}{R}\frac{dx}{R}, \tag{10}$$

where C_D is the *overall* drag coefficient. It can be shown that the correlation term $\overline{u'v'}$ approximates to the form $(lk^{\frac{1}{2}})\,\partial\bar{u}/\partial r$, which is the Prandtl expression for the shear stress, where k and l are *local* values of the turbulence characteristics. Thus

$$C_D \sim 8\iint \left(\frac{lk^{\frac{1}{2}}}{DU}\right)\left(\frac{\partial\bar{u}/U}{\partial r/R}\right)^2 \frac{r}{R}\frac{dr}{R}\frac{dx}{R}. \tag{11}$$

In smooth flow, C_D is well known to be constant over a wide range of Re. According to Bearman (1971), C_D is also constant for a given level of free-stream turbulence. The mean streamline pattern (which influences the distribution of $\partial\bar{u}/\partial r$) is dependent on the free-stream turbulence parameters in the same way as f_1 in the earlier discussion. Therefore (11) can be written as

$$C_D = G_1'\{l_f k_f^{\frac{1}{2}}/DU\}. \tag{12}$$

Variations in C_D with $l_f k_f^{\frac{1}{2}}/DU$ are due almost entirely to variations in the base pressure coefficient (Bearman 1971), so

$$C_{pb} = G_2\{l_f k_f^{\frac{1}{2}}/DU\}, \tag{13}$$

which is consistent with the dimensional analysis.

As a result of these analyses, it was decided to measure H and C_{pb} experimentally as functions of the turbulence parameter

$$\Lambda \equiv l_f k_f^{\frac{1}{2}}/DU.$$

3. Experimental

The experiments were carried out in an open-cycle, low-speed, low-turbulence wind tunnel with experimental disks suspended in the throat of the working section by piano wires. Each disk had a 30° bevelled edge, and geometrical similarity was maintained from one disk to another.

The apparatus and experimental techniques used in obtaining H have already been fully described elsewhere by Humphries & Vincent (1976). Fail *et al.* (1959) showed experimentally that the base pressure is distributed uniformly across the rear face of a disk in smooth flow. Bearman (1971) confirmed this result for both smooth and turbulent flow. On this evidence, the present experiments to measure the base pressure coefficient employed a single pressure tap at the centre of the downstream face of each disk, connected to one arm of a capacitative micromanometer. The static pressure was taken from the appropriate arm of a Pitot–static tube which also served to measure the velocity head required for determining C_{pb}. The free-stream static pressure in the wind tunnel was found to vary substantially from one part of the working section to another. Therefore, for each value of C_{pb} recorded, readings for each of the pressure differences of interest were made with the Pitot–static tube placed at many locations on a mesh in the plane containing the disk, and were averaged. Since the pressure differences measured were subject to a certain amount of fluctuation, time-averaged values were obtained by electronically integrating the electrical output signal from the micromanometer. Since all the free-stream measurements were made in the plane of the disk, no blockage correction was necessary in the calculation of C_{pb}. Justification of this overall procedure was confirmed by the fact that C_{pb} was found to be equal to $-0{\cdot}36$ (to within $\pm 1\%$) for all the disks used under smooth flow conditions, in close agreement with the measurements of Fail *et al.* (1959) and Bearman (1971).

During normal operation, good smooth flow conditions prevailed in the working section of the wind tunnel. Turbulent free-stream conditions were obtained by the use of lattice-type screens placed across the inlet to the working section. Two such screens were separately employed, with bar widths 1 and 4 cm respectively, and with screen solidity less than 50 % in both cases. The empirical data of Baines & Peterson (1951) were used to determine the intensity and length scale of the free-stream turbulence thus generated at various distances downstream from the screen. The actual turbulence quantities obtained in this way were the velocity of turbulent fluctuations parallel to and the length scale perpendicular to the axis of the experimental disk; say u'_f and l_{fr} respectively. Thus the experimental turbulence parameter, say $\Lambda_{\text{exp}} \equiv l_{fr} u'_f / DU$, was determined in the plane containing the disk, and could be varied by a combination of changing the screen and moving the experimental disk with respect to the screen. It is recognized that the mechanisms relevant to the present study cannot be confined to a single plane downstream from the turbulence-creating grid, and that the induced free-stream turbulence conditions might vary noticeably over the downstream extent of the disk wake bubble. However, for the range of conditions of the experiments reported, the estimated variation of Λ_{exp} over the downstream extent of the bubble region was always less than a few per cent of the value taken in the plane of the disk. For the purpose of subsequent discussion it is reasonable to assume a simple linear relationship between the experimental turbulence parameter Λ_{exp} and the corresponding theoretical turbulence parameter Λ. In all the experiments reported in this paper, the length scale of the free-stream turbulence was small compared with the disk diameter.

Experiments to locate the shape and position of the bubble boundary were performed using a smoke probe under visual observation, in the absence of more sophisticated suitable instrumentation at the time of the experiments. The probe was carried in a stand which in turn was free to ride along a straight track. The probe was set up and the track aligned such that the probe head could be moved axially in the wake of the experimental disk. By thus adjusting the smoke probe and carefully observing the movement of the smoke emitted, it was possible after some practice to locate the downstream (axial) extremity, or stagnation point, of the wake bubble to an accuracy of better than $\pm 0{\cdot}5$ cm for all the experimental disks used. Construction of the rest of the bubble boundary was achieved by placing the smoke-probe head just inside the bubble's downstream stagnation point and visually observing the shape of the enclosed volume of smoke. Thus it was possible to construct the bubble boundary fairly accurately over a downstream extent of up to one disk diameter, beyond which turbulent mixing had

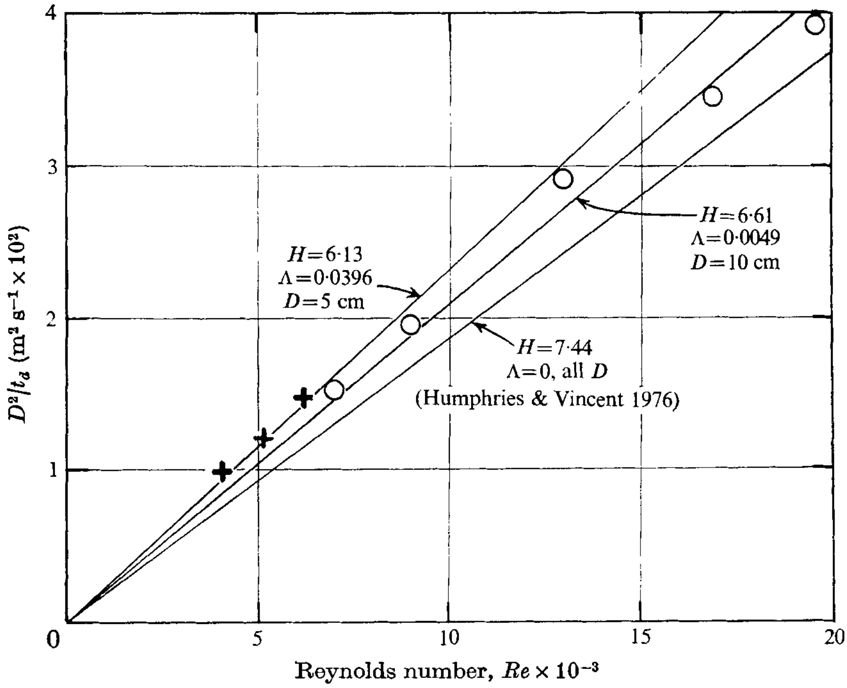

FIGURE 1. Experimental plot of D^2/t_d as a function of Reynolds number for various values of free-stream turbulence parameter.

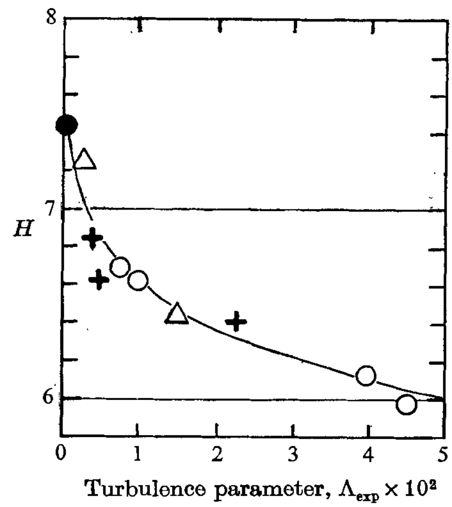

FIGURE 2. H as a function of free-stream turbulence parameter. ○, D = 5 cm; +, D = 10 cm; △, D = 15 cm; ●, all values of D.

become so intense as to prevent further reliable observation of the limiting streamline in this way. However, with this limited information together with fair knowledge of the downstream stagnation point, it was possible, by extrapolation, to build up an acceptable picture of the bubble boundary.

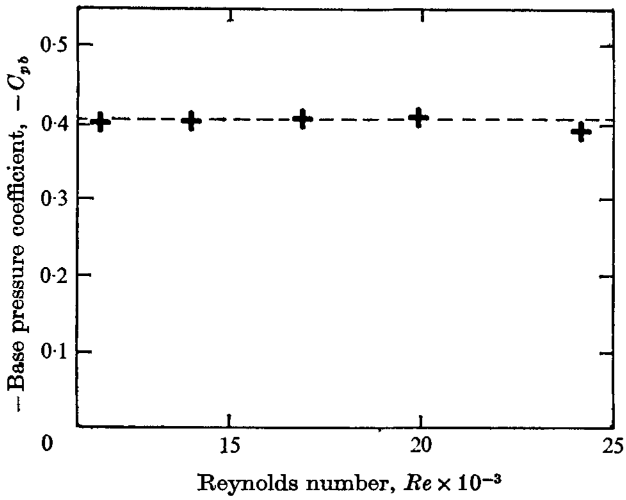

FIGURE 3. Base pressure coefficient as a function of Reynolds number for a fixed value of the free-stream turbulence parameter ($\Lambda_{exp} = 0{\cdot}049$) and $D = 10$ cm.

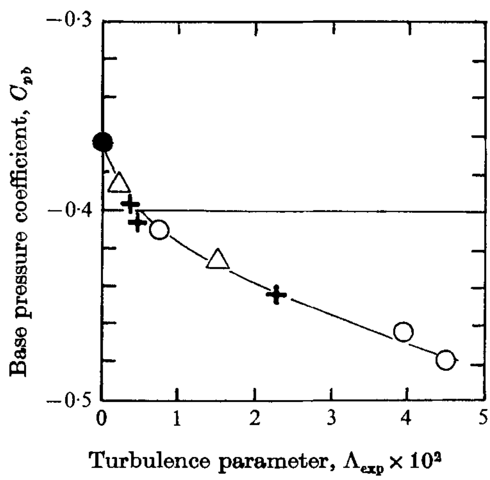

FIGURE 4. Base pressure coefficient as a function of free-stream turbulence parameter. ○, $D = 5$ cm; +, $D = 10$ cm; △, $D = 15$ cm; ●, all values of D.

4. Results and discussion

For a given set of free-stream turbulence conditions, H was determined from the slope of the experimental curve relating D^2/t_d with Re, in the manner described previously by Humphries & Vincent (1976). Some typical data for various disk sizes and experimental turbulence parameters Λ_{exp} are displayed in figure 1, each point on the graph representing the average value of the detention time taken from between 6 and 10 separate measurements. Despite some scatter in the data resulting from the fact that the wake bubble behind the disk is not truly stable but is subject to (apparently) arbitrary shedding of sizeable 'lumps' of vorticity, the curves may be reasonably concluded to be straight lines. This shows that H is independent of Re for the range of Λ_{exp} covered in the experiment.

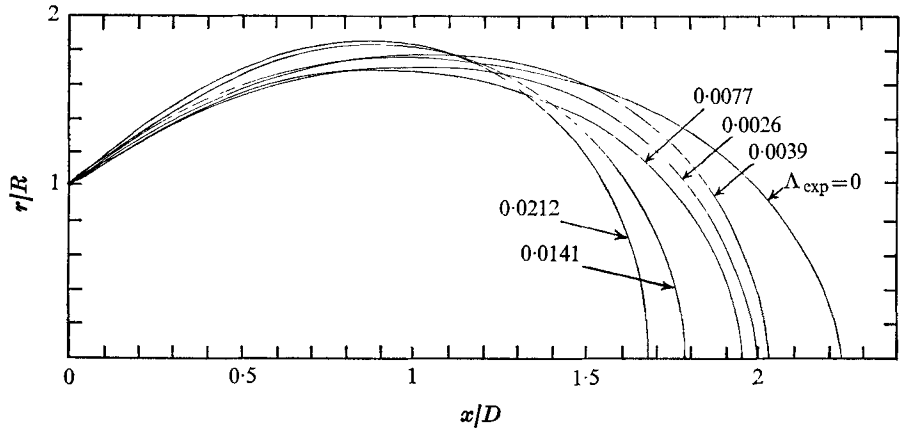

FIGURE 5. Experimentally determined wake-bubble boundaries for various values of free-stream turbulence parameter.

H was determined in this way for disks of diameter 5, 10 and 15 cm, and for Λ_{exp} up to about 0·045. The standard experimental error in each determination of H was about $\pm 7\,\%$. The results are plotted in figure 2, and it may be seen that H is uniquely determined by Λ_{exp}, confirming the general functional statement in (5) and therefore providing support for the assumptions leading up to it. H decreases as the turbulence level increases, as expected, since the enhanced mixing in the shear layer causes greater entrainment of fluid (and smoke) out of the wake bubble and so increases the dilution rate of trapped smoke when the source is removed (hence decreasing t_d).

The base pressure coefficient C_{pb} is plotted as a function of Re for fixed Λ_{exp} in figure 3, and is seen to be constant. In figure 4, C_{pb} is plotted as a function of Λ_{exp} for various disk diameters, and the good uniqueness of the relationship between the plotted quantities indicates strong support for (13). For an increasing level of turbulence, C_{pb} becomes more and more negative as the increased mixing in the shear layers of the wake bubble causes greater entrainment of fluid out of the bubble and so increases the suction experienced by the rear face of the disk. It is worth remarking that the choice of turbulence parameter in the present case is at variance with Bearman (1971), who suggested that the slightly different form $l_f^2 k_f^{\frac{1}{2}}/D^2U$ is the proper parameter for collapsing data on the base pressure coefficient. However this choice of turbulence parameter is based on dimensional analysis which appears to be in error. We suggest that the present choice of parameter is more satisfying on physical grounds.

From all that has been said so far, it is reasonable to expect a strong correlation between H and C_{pb}. We now attempt to examine the physical basis of that relationship. On the basis of the experimental evidence, for turbulent flow (3) can be rewritten in the form

$$H = f_1\left(\frac{l_c k_c^{\frac{1}{2}}}{DU}\right) f_2\left(\frac{l_c k_c^{\frac{1}{2}}}{DU}\right) \bigg/ (2b)^{\frac{1}{2}}\, \frac{l_c k_c^{\frac{1}{2}}}{DU}. \tag{14}$$

The overall drag force on the disk is associated with the shear stresses, which control the flow streamline pattern and hence the shape of the bubble boundary,

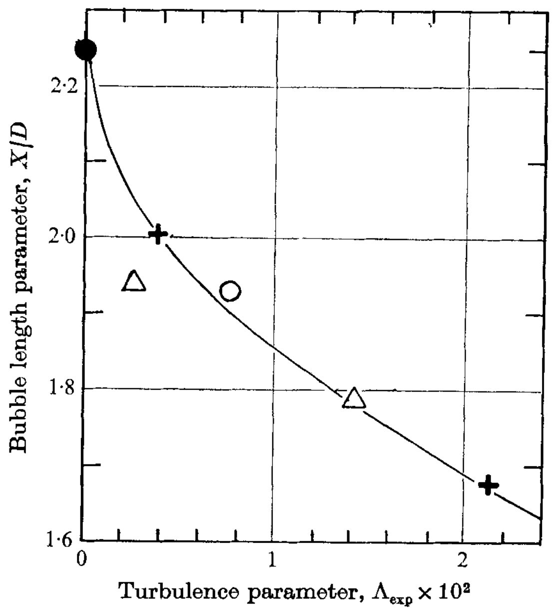

FIGURE 6. Bubble length parameter as a function of free-stream turbulence parameter. ○, D = 5 cm; +, D = 10 cm; △, D = 15 cm; ●, all values of D.

so we ought to be able to write the shape factor f_1 in terms of the drag coefficient C_D. Figure 5 shows the experimentally determined bubble boundaries for various values of Λ_{exp}, and it can be seen that the bubble shortens markedly as the level of turbulence is increased. In figure 6, the non-dimensionalized bubble *length* X/D is plotted against Λ_{exp} and is seen to vary from 2·2 to 1·68 as Λ_{exp} varies from near zero to 0·0212, appearing to follow a unique relationship for the range of disk diameters employed. In neither of these experiments did there appear to be any dependence on Re. In figure 7, values of f_1 determined from these data are plotted against Λ_{exp}, and again we obtain a unique function for all D (the maximum estimated error in f_1 is about $\pm 0{\cdot}005$). The drag coefficient is given by

$$C_D = C_{fp} + C_{Db}, \tag{15}$$

where C_{fp} is the face pressure coefficient, constant for a wide range of free-stream turbulence levels (Bearman 1971), and C_{Db} is the base drag coefficient ($= -C_{pb}$ for the normal disk). Therefore, for a given value of Λ_{exp}, C_D can be calculated directly from the measurements of C_{pb} in figure 4, assuming $C_D = 1{\cdot}12$ for smooth flow (Fail *et al.* 1959). Table 1 shows the experimental variation of f_1 with C_D, and it can be seen that the product $f_1 C_D$ is constant within the limits of experimental error over the range of conditions of the experiment.

For varying free-stream turbulence, f_2 is controlled by the characteristic coefficient of diffusion along the bubble boundary, $l_c k_c^{\frac{1}{2}}/DU$, and by X/D. Since $l_c k_c^{\frac{1}{2}}/DU$ increases with Λ_{exp} while X/D decreases (see figure 6), the net effect will be weak dependence of f_2 on Λ_{exp}. If we assume on this basis that f_2 is roughly

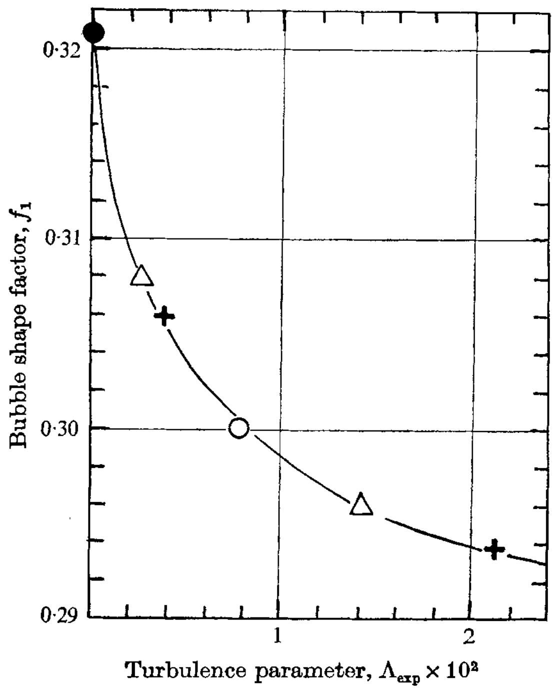

FIGURE 7. Bubble shape factor as a function of free-stream turbulence parameter. ○, D = 5 cm; +, D = 10 cm; △, D = 15 cm; ●, all values of D.

Disk diameter D (cm)	Free-stream turbulence parameter $\Lambda_{exp} \equiv l_{fr}u'_f/DU$	Bubble shape factor f_1	Disk drag coefficient C_D	f_1C_D
5, 10, 15	0	0·321	1·122	0·360
15	0·0026	0·308	1·147	0·353
10	0·0039	0·306	1·155	0·353
5	0·0077	0·300	1·168	0·350
15	0·0141	0·296	1·184	0·350
10	0·0212	0·294	1·199	0·352

TABLE 1. Drag coefficient and bubble shape factor as functions of free-stream turbulence parameter

constant, then (14) becomes

$$H \propto \frac{1}{l_c k_c^{\frac{1}{2}}/DU} \frac{1}{C_D}. \tag{16}$$

The drag coefficient as described by (11) can be evaluated in terms of the characteristic wake properties, so that

$$C_D \propto \frac{l_c k_c^{\frac{1}{2}}}{DU} \iint \left(\frac{\partial \bar{u}/U}{\partial (r/R)}\right)^2 \frac{r}{R} \frac{dr}{R} \frac{dx}{R}. \tag{17}$$

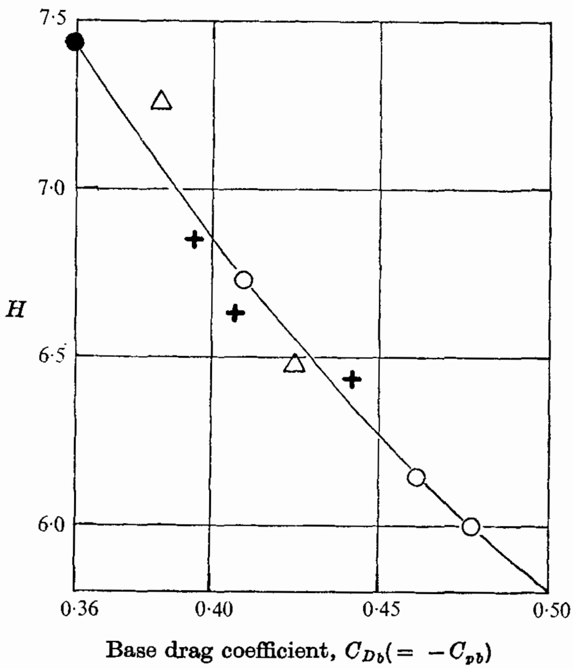

FIGURE 8. Graph to show the relationship between H and base drag coefficient. ○, D = 5 cm; +, D = 10 cm; △, D = 15 cm; ●, all values of D. ——, $H = 9{\cdot}15/(C_{Db}+0{\cdot}76)^2$.

Consider the double-integral part of this expression. As $l_c k_c^{\frac{1}{2}}/DU$ increases owing to the increase in free-stream turbulence, the effective volume of integration decreases (being related to the change in bubble volume). But at the same time recirculation velocities inside the bubble increase, so that radial velocity gradients also increase. These two effects will tend to offset one another, so we might reasonably expect variations in the double-integral part of (17) to be weak. If so,

$$C_D \propto l_c k_c^{\frac{1}{2}}/DU. \tag{18}$$

From (16) and (18), we get

$$C_D = B/H^{\frac{1}{2}}, \tag{19}$$

where B is a constant of proportionality. For smooth flow, $C_D = 1{\cdot}12$, $C_{Db} = 0{\cdot}36$ and $H = 7{\cdot}44$. Therefore (19) with (15) gives

$$H = 9{\cdot}15/(C_{Db}+0{\cdot}76)^2. \tag{20}$$

The curve representing (20) is plotted alongside the experimental data in figure 8, where agreement between experiment and theory is seen to be excellent. There is therefore strong support for the argument leading to the simple relationship between H and C_{Db} (and hence C_{pb}) for disks normal to the mainstream air flow. It is likely that similar relationships will hold for flows about flat plates of different shapes which exhibit reasonable axial symmetry. To what extent these ideas can be extended to other forms of bluff-body flow must, however, await further investigation. In practical applications of the detention-time concept for helping to understand the behaviour of scalar entities in the wake regions of bluff obstacles (e.g. aerosol transport and deposition), measurement of the base pressure coefficient may often present fewer technical problems than the direct measurement of H itself. Therefore reliable expressions of the form of (20) could be of considerable practical value.

5. Conclusions

The results of these experiments lead to the following main conclusions.

(*a*) There is a free-stream turbulence parameter, $\Lambda \equiv l_f k_f^{\frac{1}{2}}/DU$, which uniquely controls all the important properties of the flow about a flat disk, in particular H (the dimensionless group describing the detention time of a given species of scalar entity trapped in the wake bubble), the base pressure coefficient, the drag coefficient and the bubble length and shape.

(*b*) As the level of turbulence increases, H decreases while the base pressure coefficient becomes more negative, from which it is seen that, for a given species of scalar entity, there is a simple unique experimental relationship between H and the base pressure coefficient. This relationship is plausible on physical grounds.

This work is supported by a Research Grant from the Science Research Council (B/RG/6177.8), who also provide a Research Studentship for one of the authors (W. H.). The authors would like to thank the Department of Architecture and Building Science at Strathclyde University for the use of their wind tunnel, and Professor E. Eisner of the Department of Applied Physics for his encouragement. Particular thanks go to Mr J. Broadfoot, Mr J. Crawley, Mr W. Fraser and Mr J. Hercus for their valuable technical assistance.

REFERENCES

Baines, W. D. & Peterson, E. G. 1951 An investigation of flow through screens. *Trans. A.S.M.E.* **73**, 467–480.

Bearman, P. W. 1971 An investigation of the forces on flat plates normal to a turbulent flow. *J. Fluid Mech.* **46**, 177–198.

Carmody, T. 1963 Establishment of the wake behind a disk. Ph.D. thesis, University of Iowa.

Carmody, T. 1964 Establishment of the wake behind a disc. *Trans. A.S.M.E.* paper 64-FE-3.

Fail, R., Lawford, J. A. & Eyre, R. C. W. 1959 Low speed experiments on the wake characteristics of flat plates normal to an air stream. *Aero. Res. Counc. R. & M.* no. 3120.

Humphries, W. & Vincent, J. H. 1976 An experimental investigation of the detention of airborne smoke in the wake bubble behind a disk. *J. Fluid Mech.* **73**, 453–464.

Launder, B. E. & Spalding, D. B. 1972 *Mathematical Models of Turbulence*. Academic.

Prandtl, L. 1945 Über ein neues Formelsystem für die ausgebildeten Turbulenz. *Nachr. Akad. Wiss. Göttingen.*

Rouse, H. 1960 Répartition de l'énergie dans les zones de décollement. *Houille Blanche*, no. 3, p. 221.